Available online at www.sciencedirect.com

ScienceDirect

journal homepage: www.elsevier.com/locate/he

Short Communication

High CO tolerance of Pt nanoparticles synthesized by sodium borohydride in a time-domain NMR spectrometer

A.S. Ramos [a], M.C.L. Santos [a], C.M. Godoi [a], L.C. de Queiroz [b], J. Nandenha [a], E.H. Fontes [a], W.R. Brito [b], M.B. Machado [b], A.O. Neto [a], R.F.B. de Souza [a,*]

[a] Instituto de Pesquisas Energéticas e Nuclears, IPEN/CNEN-SP, Av. Prof. Lineu Prestes, 2242 Cidade Universitária, CEP 05508-900, São Paulo, SP, Brazil

[b] Central Analytica, Universidade Federal Do Amazonas, UFAM, Av. General Rodrigo Octavio Jordão Ramos, 1200 - Coroado I, Manaus, 69067-005, AM, Brazil

HIGHLIGHTS

- Nanoparticle synthesis by sodium borohydride within a TD-NMR spectrometer.
- High CO tolerance of Pt/C due to lattice parameter contraction.
- Pt/C MFP90° has the better performance over H_2 and H_2 + CO experiments.

GRAPHICAL ABSTRACT

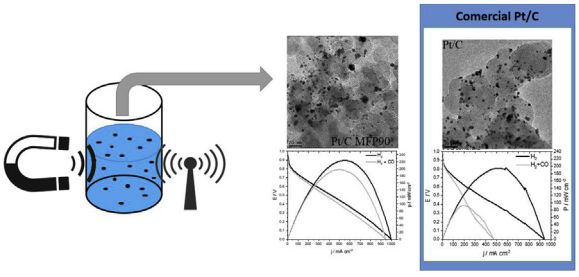

ARTICLE INFO

Article history:
Received 23 April 2020
Received in revised form
9 June 2020
Accepted 11 June 2020
Available online 25 July 2020

Keywords:
Pt/C
CO stripping
Fuel cell

ABSTRACT

The CO poisoning effect was overcome using a novel synthesis method. This method consists of using sodium borohydride reducing agent assisted by magnetic field and radiofrequency pulses in the time-domain NMR spectrometer. This synthesis was useful to disperse the Pt nanoparticles over the carbon support and to compress the lattice strain of the Pt crystalline structure. Besides that, Pt/C MFP90° showed a multi-CO oxidation component in cyclic voltammetry, and this can avoid the poisoning effect by creating a large availability of CO species to be adsorbed, desorbed, and re-adsorbed. Pt/C MFP90° has also shown the best performance in the PEMFC regarding H_2 and CO + H_2 experiments.

* Corresponding author.
E-mail address: souza.rfb@gmail.com (R.F.B. de Souza).

https://doi.org/10.1016/j.ijhydene.2020.06.105

Time domain NMR
Nuclear magnetic resonance

Introduction

Adsorption of carbon monoxide on Pt active sites is considered one of the significant drawbacks considering the use of Pt in proton exchange membrane fuel cells (PEMFC). For instance, CO can block the active platinum sites required for hydrogen electrosorption and, consequently, decrease the fuel cell performance [1–3].

There are several attempts to avoid CO poisoning on Pt active sites, the general approach is to weaken the adsorption interaction energy between CO and the Pt active site [4]. The electrocatalyst design is fundamental to tune the interaction above. One of the most common ways to do this is to synthesize alloy electrocatalysts containing Pt [2,5]. Among the alloy electrocatalysts studied along with Pt, stands out Ir, Te, Cu, Fe and Rh. They have the purpose of altering the CO adsorption energies sites of Pt nanoparticles [6]. A way to synthesize alloy electrocatalysts is to use sodium borohydride as a reducing agent [7,8]. Other tactics to improve CO tolerance involves the use of co-catalysts, such as transition metal oxides, nitrides, carbides, and phosphides [6].

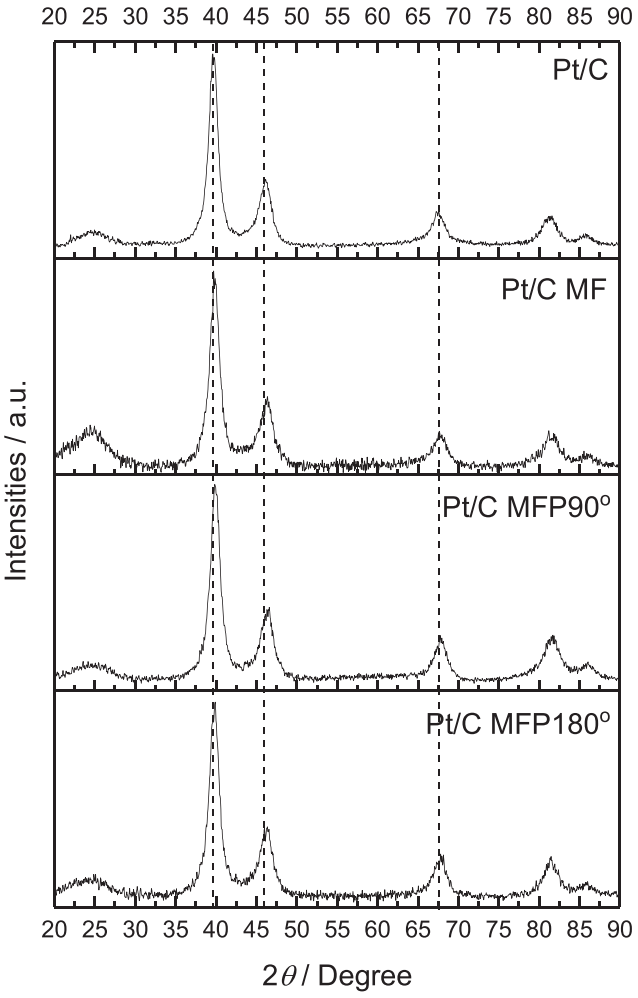

Fig. 1 – X-ray diffraction pattern of Pt/C, Pt/C MF, Pt/C MFP90° and Pt/C MFP180°.

Another approach is to change the tensile strain of Pt crystalline structure, which will cause a d-band center variation and, consequently, the lowering of CO adsorption energy [9]. Then, the design of core-shell nanoparticles and bimetallic alloys has shown crucial in that sense [1,10]. So, our novel synthesis method consists in use sodium borohydride reducing agent assisted by a magnetic field and radiofrequency pulses. This might produce changes in the electronic structure of the electrocatalysts and so improving the CO tolerance.

In a PEMFC, the use of a second metal in an electrocatalyst generally tend to be unstable because of the surrounding medium [11]. Furthermore, the design of core-shell nanoparticles tends to involve several steps in the synthesis, which turns out to be impracticable in more massive production. Therefore, this work aims to employ the sodium borohydride synthesis [12] within a time-domain NMR spectrometer studying the influence of the magnetic field with radio frequency pulses during the electrocatalysts synthesis, and finally, evaluate the CO and H_2 oxidation process.

Materials and methods

All the Pt based electrocatalysts (20 wt% of metals loading) electrocatalysts were prepared using $H_2PtCl_6.H_2O$ (Aldrich) in a mixture of ultrapure water and isopropanol (Merck) (50/50). The vulcan Carbon XC72 (cabot) was used as support. The synthesis was performed in a time-domain NMR spectrometer Specific 15 MHz (Fine Instrument Technology-FIT) with a 0.33 T magnetic field. Three different synthesis conditions of time-domain nuclear magnetic resonance were applied: the magnetic field without a radiofrequency pulse, only under magnetic field influence (Pt/C MF), the magnetic field with 90°pulse (Pt/C MPF90°), and the magnetic field with 180°pulse (Pt/C MFP180°). The $NaBH_4$ (Aldrich) solution was added while the radiofrequency pulse was applied. The pulse duration was set to 0.5 ms (for Magnetic Field and Pulse 90°-or MFP90°) and 1.0 ms (for Magnetic Field and Pulse 180°-or MFP180°) with 80% of power and with 3.0 s of the time interval between the pulses, a total of 300 pulses.

All Pt/C electrocatalysts were characterized by X-ray diffraction (XRD) using the Rigaku diffractometer model Miniflex II with Cu Kα radiation source (l = 0.15406 nm). The diffractograms were recorded from 2θ = 20° to 90° with a step size of 0.05° and a scan time of 2 s per step. Transmission electron microscopy (TEM) was carried out using the JEOL JEM-2100 electron microscope operated at 200 kV. The mean

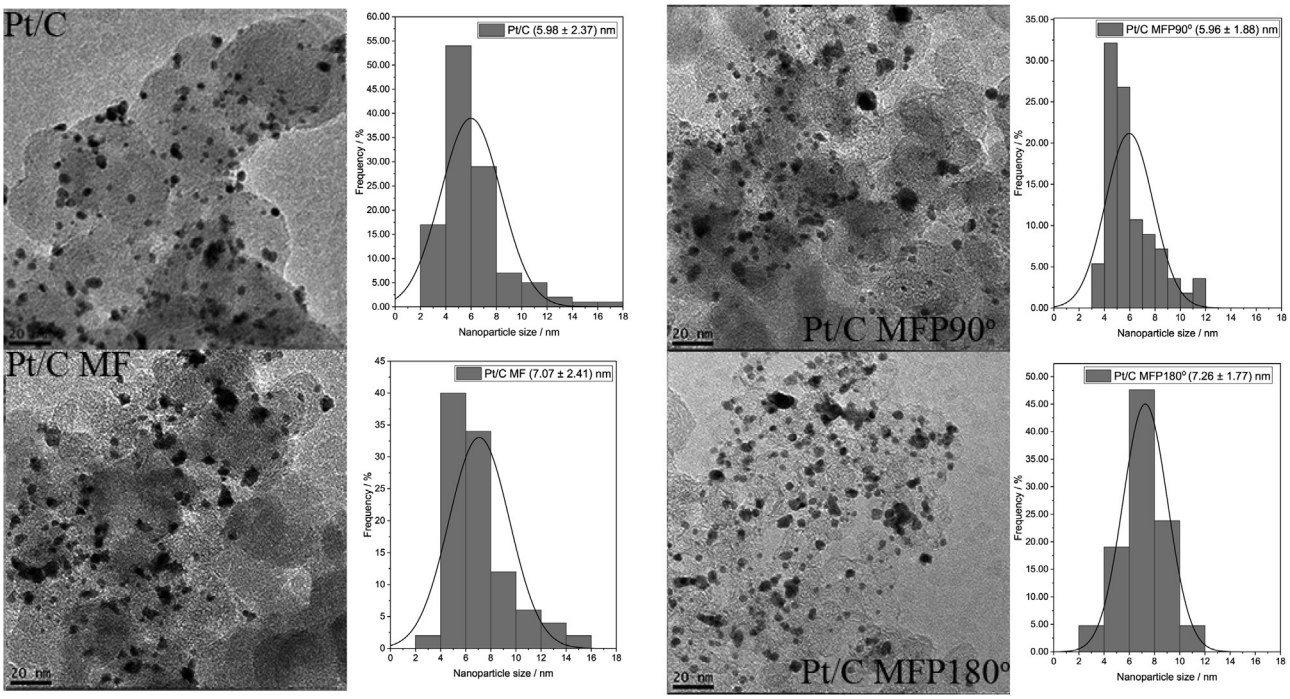

Fig. 2 – Transmission electron microscopy and nanoparticle size distribution of Pt/C, Pt/C 0°, Pt/C 90° and Pt/C 180°.

particle sizes were determined by counting more than 200 particles from different regions of each sample.

The cyclic voltammetry measurements were carried at 25 °C using an Autolab PGSTAT 302 potentiostat/galvanostat. The working electrode is a carbon vitreous with porous ultra-thin layer deposited [13], the reference electrode was the reversible hydrogen electrode (RHE), and the counter electrode was a Pt plate. The electrochemical measurements were done in the presence of 0.5 mol L^{-1} H_2SO_4 solutions saturated with N_2. For CO-stripping, the solution was purged with N_2 in the working electrode for 30 min, and then purified with CO gas for 30 min, and the working electrode potential was set to 0.2 V vs. RHE. After the adsorption, the CO was removed from the electrolyte, followed by N_2 bubbling for 15 min. The CO-stripping voltammograms were recorded at a scan rate of 10 mV s^{-1}.

The fuel cell experiments were performed using Pt/C materials synthetized as anode, using hydrogen flux (300 mL min^{-1}) and Pt/C the commercial Pt/C (BASF), using oxygen flux (200 mL min^{-1}). The tests were realized in a single cell PEMFC with an active geometric surface area of electrodes equal to 5 cm^2. For fuel cell studies also, it was utilized the carbon-cloth PTFE-treated as a gas diffusion layer and a Nafion® 117 membrane as electrolyte. The anode electrodes and the cathode prepared were made with 1 mgPt cm^{-2} electrocatalyst loading for experiments with the synthesis gas (H_2+CO) was maintained an atmospheric pressure in the anode and cathode. The fuel cell temperature was 80 °C with the H_2+CO (CO 100 ppm) flux regulated at 300 mL min^{-1} in the anode and O_2 flux at 200 mL min^{-1} in the cathode.

Results and discussion

Fig. 1 shows the X-ray diffraction of Pt/C electrocatalysts. For all of them, it is possible to identify the presence of the (002) plane characteristic of carbon (JCPDF # 50–926). Furthermore, it is also possible to notice the presence of intense peaks at ~40°, 45°, 67°, 82° and 85°, they are respectively associated with the crystalline planes (111), (200), (220), (311) and (222) of polycrystalline platinum (JCPDF # 04–802) with face-centered cubic structure (FCC).

It is possible to notice that the Pt/C nanoparticles synthesized in the NMR spectrometer a small shift in 2θ for more positive angles, and this leads to a contraction of the lattice parameter. The lattice parameter calculation considering the (220) crystalline plane is the following [14]. The lattice parameter value of 0.392 nm found for Pt/C is following the Pt bulk reported in Kelly [15], for Pt/C MF and MFP180° is 0.391 nm, and Pt/C MFP90° is 0.390 nm. It is noteworthy to mention that the highest lattice parameter contraction observed was for Pt/C MFP90°. Therefore, for Pt/C MFP90°, we expect to have a superposition of the atomic orbitals in a way that the d-band center of the surface atoms tends to go further from the Fermi level. Furthermore, the Pt atoms are probably closer to each other than (111) surface. The overlap matrix elements and hence the d-bandwidth are therefore larger significant, the d-bands are lower in energy, and consequently, these reconstructed Pt surfaces bind CO weaker [16].

The micrographs in Fig. 2 show the distribution of the Pt nanoparticles over the carbon support. All of them are well dispersed over the carbon support, but still, some

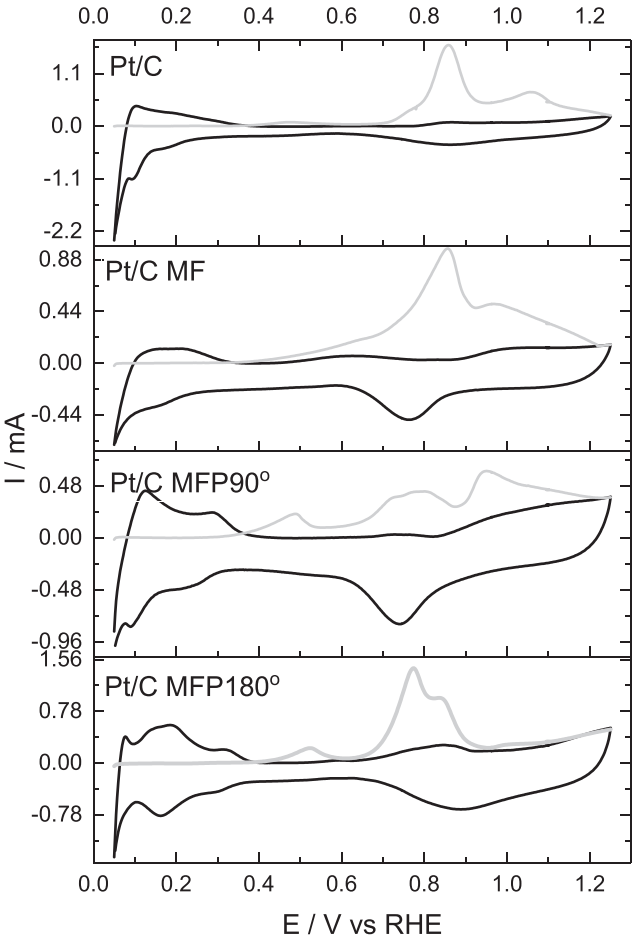

Fig. 3 – black curves corresponding the cyclic voltammetry on Pt/C, Pt/C MF, Pt/C MFP90°, and Pt/C MFP180°, in 0.5 mol L^{-1} H_2SO_4, and the gray curve represents the CO stripping.

nanoparticles agglomeration occurred. The morphological characteristics of the Pt nanoparticles, as well as the mean diameters, are consistent with reported in rhe literature [17–19]. Regarding the shape of the nanoparticle size distribution is attributed to the sodium borohydride reducing agent [20].

Pt/C MFP90° has a smaller mean diameter nanoparticle size, this means that Pt/C MFP90° has the highest nanoparticle surface area, since the surface/volume ratio R is R = 6/d, where d is the nanoparticle mean diameter [21], this also means that Pt/C MFP90° could have the highest electrochemical activity.

Fig. 3 shows the characteristic voltammetry pattern of Pt/C nanoparticles with turn in and out CO in 0.5 mol L^{-1} H_2SO_4. Without CO (black line), it is possible to observe a good definition in the adsorption and desorption region of hydrogen (0.05–0.4 V), the sharpness and the symmetry of the adsorption profile for each material are different due to the composition of faces present at the electrode interface with the solution [22]. Pt/C MFP90° and Pt/C MFP180° have profiles like materials with a predominance of faces on the surface (100) [23] and (110) [24]. In Pt/C, that is a polycrystalline structure on Carbon Vulcan XC72, regarding CO voltammetry, the most intense peak has been observed at 0.85 V and 1.05 V in agreement with the work of Ciapina et al. [25]. The shoulder peak at 0.79 V was attributed to an inter-particle effect, which is an interaction between CO and OH species adsorbed in different nanoparticles, and this effect is proportional to the anchorage of Pt nanoparticles on the carbon support [25].

All the other electrocatalysts show different shapes regarding CO cyclic voltammetry. Pt/C MF present form like the Pt/C, but the 1.05 V peak position is shifted to 0.95 V in according with Ciapina corresponding to face (111) [25]. Furthermore, the CO oxidation peak intensity of Pt/C MF in 0.85 V is relatively smaller than Pt/C. For Pt/C MFP 180° showed peaks close for Pt/C MF, with the addition of the pre-peak of CO oxidation at 0.5 V, that appear when the oxidation of adsorbed CO at step sites [26], however the peak at 0.75 V is more intense than the peak at 0.85 V, and the peak at 0.95 V can hardly be observed.

In Pt/C MFP 90° the CO oxidation shows a pre-peak at ~0.5 V, also present at 0.7 V, 0.85 V, and 0.95 V and, it is less intense and broader (0.85 V) than in the other materials, which can be explained by i) a difference in the metal/support interaction shifting the potentials of CO oxidation [27,28]; ii) due to defects and adlayers of different faces [29,30] caused by the electromagnetic pulses. This multipeak oxidation process can show to us a large availability of active sites. It shows that CO is easily oxidized in this electrocatalyst, indicating good tolerance to the CO poisoning effect. Therefore, the time-domain NMR synthesis alters the electronic structure of the Pt/C MFP electrocatalysts.

Fig. 4 shows the polarization and power density curves for Pt/C MFP catalysts and Pt/C. Pt/C has an open circuit voltage of 970 mV in contrast to 950 mV of all the others, regarding both conditions (H_2 and H_2+CO). The maximum power density obtained for Pt/C regarding H_2 experiment is 194 mW cm^{-2} and 92 mW cm^{-2} for H_2+CO, a decrease of 52% in power. Pt/C MF has the maximum power density of 196 mW cm^{-2} for H_2 and 90 mW cm^{-2} for H_2+CO (decrease of 54%). Pt/C MFP 90° has the maximum power density of 224 mW cm^{-2} for H_2 and 197 mW cm^{-2} for H_2+CO (decrease of 12%) and Pt/C MFP180° has the maximum power density of 190 mW cm^{-2} for H_2 and 97 mW cm^{-2} for H_2+CO (decrease of 48%). Furthermore, Pt/C 90° has the highest final current density in the polarization curve experiment.

The performance in the PEMFC experiment regarding Pt/C MFP 90° is mainly attributed to the high CO tolerance that this electrocatalyst present. The mechanism of CO oxidation over Pt active sites is a Langmuir-Hinshelwood type and is described below [25]:

$$H_2O + Pt \leftrightarrow Pt - OH_{ads} + H^+ + e^- \quad (1)$$

$$Pt - CO_{ads} + Pt - OH_{ads} \rightarrow CO_2 + H^+ + e^- + 2Pt \quad (2)$$

Furthermore, the reaction rate in eq. (1) is not compromised by the CO poisoning, due to the possibility of OH adsorbed species oxidize CO to CO_2. Besides, the electronic effect caused by the novel synthesis method can weaken the Pt-CO_{ads} bond in (2) which turns out to facilitate the oxidation

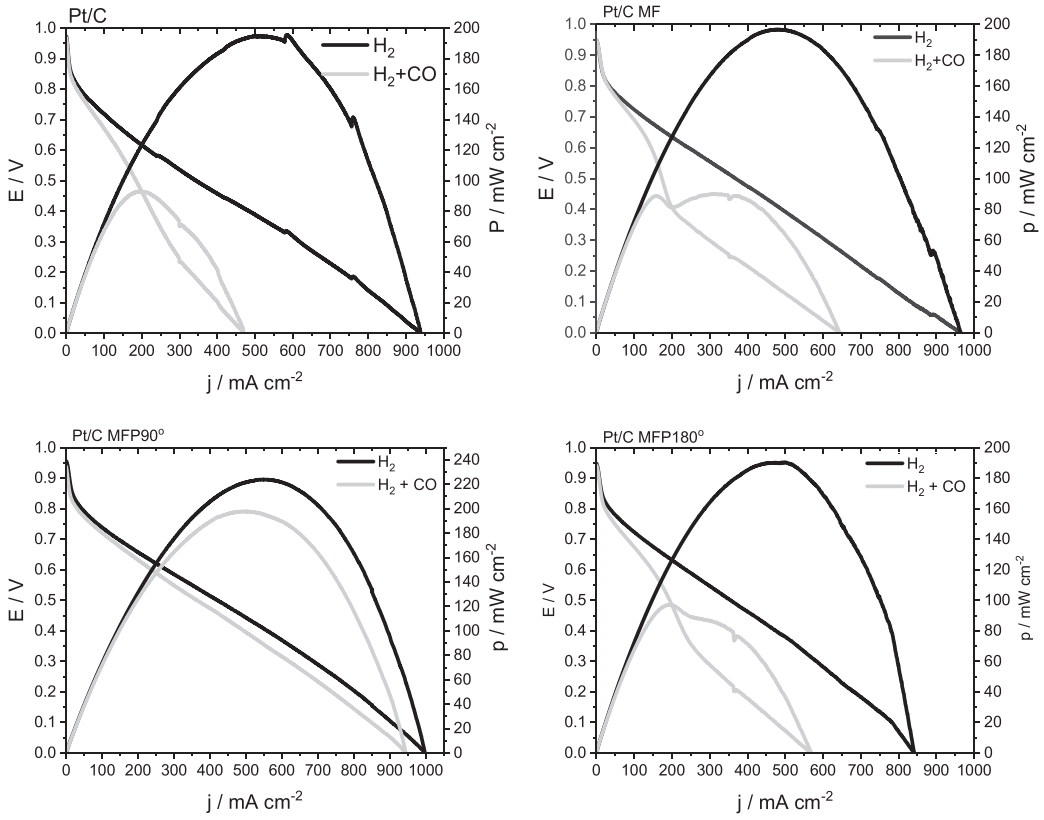

Fig. 4 – Pt/C, Pt/C Field 0°, Pt/C MFP 90° and Pt/C Field 180° Fuel Cell experiment. The black lines represent the H_2 experiment and the gray lines H_2 + CO experiment.

through OH_{ads} to CO_2. It means that the slightest loss of power due to the presence of CO can be explained by the existence of a surface defect, adlayers of different faces and/or strongly interaction metal/support, creating a multi CO oxidation process. That is oxidized to various potentials while scanning potentials, as noted in voltammetry (Fig. 3), and thereby reducing the effect of poisoning, thus influencing less on the power drop.

Conclusion

The Time Domain NMR synthesis was advantageous to create lattice strain compression in Pt crystallographic structure and, then, probably weakening the CO adsorption energy on Pt/C MFP90°. In addition, this latter electrocatalyst showed the smallest average diameter size, which turns out to be extremely useful to oxidize CO species. The cyclic voltammetry revealed a multi-CO oxidation process, which turns out to be incredibly effective in increasing the availability of active sites for water, H_2, and CO to be adsorbed.

The PEMFC experiment also showed excellent performance of Pt/C MFP90° in comparison with the other electrocatalysts studied. This behavior could be explained due to the possibility of metal/support interaction wich activated water and surface adlayers, and defects shifted the CO oxidation for lower potentials. However, new studies yet are necessary using Raman spectroscopy, XPS, XANES/EXAFS and DFT calculations can help to elucidate differences in the metal/support interaction.

Declaration of competing interest

The authors declare that they have no known competing financial interests or personal relationships that could have appeared to influence the work reported in this paper.

Acknowledgements

The authors thank the CAPES, FAPESP (2014/09087–4, 2014/50279–4, 2017/11937, CNPq (300816/2016–2 and 429727/2018–6), Financiamento de Estudos de Projets e Programs-FINEP and Analytical Center of UFAM for financial support and infrastructure for the financial support.

REFERENCES

[1] He J, Shen Y, Yang M, Zhang H, Deng Q, Ding Y. The effect of surface strain on the CO-poisoned surface of Pt electrode for hydrogen adsorption. J Catal 2017;350:212–7.
[2] Ren H, Humbert MP, Menning CA, Chen JG, Shu Y, Singh UG, et al. Inhibition of coking and CO poisoning of Pt catalysts by

the formation of Au/Pt bimetallic surfaces. Appl Catal Gen 2010;375:303–9.
[3] Trens P, Durand R, Coq B, Coutanceau C, Rousseau S, Lamy C. Poisoning of Pt/C catalysts by CO and its consequences over the kinetics of hydrogen chemisorption. Appl Catal B Environ 2009;92:280–4.
[4] Ozdemir MO, Pasaogullari U. Modeling the oscillative behavior and carbon monoxide removal by current pulsing technique in H2/CO mixtures for Pt catalyst layer. Int J Hydrogen Energy 2016;41:10854–69.
[5] Yang Z, Nagashima A, Fujigaya T, Nakashima N. Electrocatalyst composed of platinum nanoparticles deposited on doubly polymer-coated carbon nanotubes shows a high CO-tolerance in methanol oxidation reaction. Int J Hydrogen Energy 2016;41:19182–90.
[6] Wei D, Ma L, Gan M, Han S, Shen J, Ding J, et al. Pt-based catalyst decorated by bimetallic FeNi2P with outstanding CO tolerance and catalytic activity for methanol electrooxidation. Int J Hydrogen Energy 2020;45:4875–86.
[7] Lu W, Liu T, Xie L, Tang C, Liu D, Hao S, et al. In situ derived Co B nanoarray: a high-efficiency and durable 3D bifunctional electrocatalyst for overall alkaline water splitting. Small 2017;13:1700805.
[8] Li K, Ma M, Xie L, Yao Y, Kong R, Du G, et al. Monolithically integrated NiCoP nanosheet array on Ti mesh: an efficient and reusable catalyst in NaBH4 alkaline media toward on-demand hydrogen generation. Int J Hydrogen Energy 2017;42:19028–34.
[9] Kheradmandinia S, Khandan N, Eikani MH. Two-layer anode electrode with non-noble catalysts as CO tolerant structure for PEM fuel cell. Int J Hydrogen Energy 2019. https://doi.org/10.1016/j.ijhydene.2019.09.031.
[10] Dehcheshmeh MS, Kiani A. Synthesis of Pt nano catalyst in the presence of carbon monoxide: superior activity towards hydrogen evolution reaction. Int J Hydrogen Energy 2019;44:23969–74.
[11] Akhairi MAF, Kamarudin SK. Catalysts in direct ethanol fuel cell (DEFC): an overview. Int J Hydrogen Energy 2016;41:4214–28.
[12] Piasentin RM, Spinacé EV, Tusi MM, Neto AO. Preparation of PdPtSn/C-Sb2O5. SnO2 electrocatalysts by borohydride reduction for ethanol electro-oxidation in alkaline medium. Int J Electrochem Sci 2011;6:2255–63.
[13] De Souza RFB, Silva JCM, Simoes FC, Calegaro ML, Neto AO, Santos MC. New approaches for the ethanol oxidation reaction of Pt/C on carbon cloth using ATR-FTIR. International Journal of Electrochemical Science 2012;7:5356–66.
[14] Wei M, Huang L, Huang S, Chen Z, Lyu D, Zhang X, et al. Highly efficient Pt-Co alloy hollow spheres with ultra-thin shells synthesized via Co-B-O complex as intermediates for hydrogen evolution reaction. J Catal 2020;381:385–94.
[15] Kelly BG, Loether AB, DiChiara AD, Henning RW, DeCamp MF, Unruh KM. Lattice parameter evolution in Pt nanoparticles during photo-thermally induced sintering and grain growth. J Phys Chem Solid 2017;108:104–8.
[16] Nilsson A, Pettersson LGM. Chapter 2 - adsorbate electronic structure and bonding on metal surfaces. In: Nilsson A, Pettersson LGM, Nørskov JK, editors. Chemical bonding at surfaces and interfaces. Amsterdam: Elsevier; 2008. p. 57–142.
[17] Fontes EH, Piasentin RM, Ayoub JMS, da Silva JCM, Assumpção MHMT, Spinacé EV, et al. Electrochemical and in situ ATR-FTIR studies of ethanol electro-oxidation in alkaline medium using PtRh/C electrocatalysts. Materials for Renewable and Sustainable Energy 2015;4:3.
[18] Bayrakçeken A, Türker L, Eroğlu I. Improvement of carbon dioxide tolerance of PEMFC electrocatalyst by using microwave irradiation technique. Int J Hydrogen Energy 2008;33:7527–37.
[19] Samad S, Loh KS, Wong WY, Lee TK, Sunarso J, Chong ST, et al. Carbon and non-carbon support materials for platinum-based catalysts in fuel cells. Int J Hydrogen Energy 2018;43:7823–54.
[20] Assumpção MHMT, Piasentin RM, Hammer P, De Souza RFB, Buzzo GS, Santos MC, et al. Oxidation of ammonia using PtRh/C electrocatalysts: fuel cell and electrochemical evaluation. Appl Catal B Environ 2015;174–175:136–44.
[21] Vollath D. Nanoparticles-Nanocomposites–Nanomaterials: An Introduction for Beginners. John Wiley & Sons; 2013.
[22] Hersbach TJP, Yanson AI, Koper MTM. Anisotropic etching of platinum electrodes at the onset of cathodic corrosion. Nat Commun 2016;7:12653.
[23] Antoniassi RM, Otubo L, Vaz JM, Oliveira Neto A, Spinacé EV. Synthesis of Pt nanoparticles with preferential (100) orientation directly on the carbon support for Direct Ethanol Fuel Cell. J Catal 2016;342:67–74.
[24] Attard GA, Hunter K, Wright E, Sharman J, Martínez-Hincapié R, Feliu JM. The voltammetry of surfaces vicinal to Pt{110}: structural complexity simplified by CO cooling. J Electroanal Chem 2017;793:137–46.
[25] Ciapina EG, Santos SF, Gonzalez ER. Electrochemical CO stripping on nanosized Pt surfaces in acid media: a review on the issue of peak multiplicity. J Electroanal Chem 2018;815:47–60.
[26] Cuesta A, Couto A, Rincón A, Pérez MC, López-Cudero A, Gutiérrez C. Potential dependence of the saturation CO coverage of Pt electrodes: the origin of the pre-peak in CO-stripping voltammograms. Part 3: Pt(poly). J Electroanal Chem 2006;586:184–95.
[27] Yang Z, Nakashima N. An electrocatalyst based on carbon nanotubes coated with poly(vinylpyrrolidone) shows a high tolerance to carbon monoxide in a direct methanol fuel cell. ChemCatChem 2016;8:600–6.
[28] Rizo R, Sebastián D, Rodríguez JL, Lázaro MJ, Pastor E. Influence of the nature of the carbon support on the activity of Pt/C catalysts for ethanol and carbon monoxide oxidation. J Catal 2017;348:22–8.
[29] Lebedeva NP, Rodes A, Feliu JM, Koper MTM, van Santen RA. Role of crystalline defects in electrocatalysis: CO adsorption and oxidation on stepped platinum electrodes as studied by in situ infrared spectroscopy. J Phys Chem B 2002;106:9863–72.
[30] Herrero E, Chen Q-S, Hernández J, Sun S-G, Feliu JM. Effects of the surface mobility on the oxidation of adsorbed CO on platinum electrodes in alkaline media. The role of the adlayer and surface defects. Phys Chem Chem Phys 2011;13:16762–71.